LANDSLIDE INVENTORY MAPPING FROM LANDSAT-8 NDVI TIME SERIES USING ADAPTIVE LANDSLIDE INTERVAL DETECTION

Tsung-Han Wen, Tee-Ann Teo*

Dept. of Civil Engineering, National Yang Ming Chiao Tung University, Hsinchu, Taiwan 30010

Commission III, ICWG III/IVa

KEYWORDS: Landslide Detection, Time Series, NDVI, Landsat-8.

ABSTRACT:
A landslide inventory map is one of the essential sources of geospatial information for land resource management. This study proposes an interval-based landslide detection strategy using satellite images' time series vegetation index. Landslide trends to be abruptly changed with the landscape can be clearly detected using the time series vegetation index. The proposed adaptive landslide interval detection (LID) method is a two stage algorithm. The first stage extracts local extremes and divides the time series to obtain discriminative intervals. Then, a predefined threshold is applied to determine whether a landslide occurs in each interval. The experiment compares the proposed scheme and the traditional time series forest (TSF) algorithm on a pre-labeled dataset. In the comparison of the results obtained from TSF and LID, the validation results show that the proposed LID has better discriminative ability in real scenarios, and the landslide detection rate for large areas reaches 85%. But the TSF can only provide good results on well-defined and unmixing datasets. In addition, LID does not require a large number of training datasets and can be applied to irregular time series with various lengths. In summary, this study demonstrated that the LID global pattern concerned splitting strategy is more effective than TSF random interval segmentation.

1. INTRODUCTION

Landslides often pose a serious threat to people, property, and the environment. The causes of landslides are complex, including earthquakes, volcanic activities, rainfall, and different kinds of human actions. As a result, it is challenging to accurately predict landslide occurrence time and location. Nevertheless, areas that have experienced large-scale landslides have a high probability of repeated landslides due to weakened geological conditions and difficulty in vegetation recovery. Landslide detection is indispensable for making a complete and accurate landslide inventory map for management.

Traditional landslide detection methods can be divided into geomorphological field surveys and visual interpretation using stereoscopic aerial photographs (Guzzetti et al., 2012). The former is limited by the available stations and can only obtain partial information; the latter requires expert experience, professional training, and a unified detection standard. Besides, the traditional method requires huge labor costs and is time-consuming.

Nowadays, large area landslide detection is mainly based on remote sensed image data, and various methods are developed according to different sensor mechanisms. For instance, satellite SAR data have been widely used to interpret slope failures (Shibayama and Yamaguchi, 2014; Handwerger et al., 2020). The use of optical remote sensing images is another mainstream for landslide detection (Danneels et al., 2007; Cheng et al.,2013; Chen et al., 2017). In addition, many studies combined both SAR and optical images for landslide investigation (Furuta and Tomiyama, 2008; Plank et al., 2016).

Most of the landslide detection methods use bitemporal satellite images, which means that they employ pre- and post-event images as the basis for detection. For example, Herrera (2019) used Sentinel-2 optical images to extract landslide diagnostic features which were computed using band rationing and subtraction of pre-/post-event images. Then Herrera combine object-based image analysis (OBIA) and machine learning algorithms to develop an automatic landslide detection method. Konishi and Suga (2017) also extracted damaged areas caused by debris flow using normalized difference sigma naught index (NDSI) from bitemporal COSMO-SkyMed images. The limitation of using bitemporal images for landslide detection is highly time-dependent. Moreover, optical image acquisition should consider cloud coverage. Besides, if the landslide area becomes bare soil and then recovers to vegetation within the selected time interval, a landslide might not be successfully detected.

Time series satellite images overcome the problem of data continuity for land cover changes in bitemporal imagery. Landslide detection using chronological observations can be regarded as binary classification of time series (Hu et al., 2018). Many time series classification (TSC) algorithms have been developed to extract useful information. Bagnall et al. (2017) classified TSC algorithms according to the types of discriminatory features as follows: (1) whole series; (2) shapelets-based; (3) dictionary-based; and (4) interval-based TSC. The whole series method, such as dynamic time warping (Müller, 2007), expects the overall behavior of the timing to be similar and therefore compensate small misalignments. The shapelet is a recognizable time series subsequences which can maximally represent a class (Ye and Keogh, 2009). It can be used for template matching on time series, for example, time-lagged cross-correlation (Shen, 2015). On the contrary, dictionary-based methods identify the repetition frequency of subseries (Schäfer, 2015).

* Corresponding author.

Instead of using entire series, the interval-based method utilizes one or more intervals to divide the time series. Discriminative features are then extracted by key intervals or by summarizing multiple intervals. Deng et al. (2013) proposed a time series forest (TSF) algorithm, employing a random forest approach with summary statistics features of each interval in time series classification. There are also several interval-based TSC algorithms like time series bag-of-features (TSBF) (Baydogan et al., 2013) and learned pattern similarity (LPS) (Baydogan and Runger 2016).

However, the characteristics of landslide time series include different occurrence times, different durations, and no regular frequency. The whole series and shapelets-based methods usually fail in time series landslide detection. We assume that an irregular landslide behavior includes three intervals: pre-event, landsliding, and post-event. Therefore, it is a more appropriate way to detect a landslide using an interval-based method. The subseries segmentation methods of TSF, TSBF and LPS are all based on random intervals without considering the global time series pattern.

In this study, we split the time series data into several intervals by every identified peak and valley of time series. Based on this, a simple landslide detection method is proposed, which can also operate on time series of arbitrary length. This discrimination procedure can be applied for landslide detection. Hence, the contribution of this research is to perform global pattern concerned landslide detection by interval-based TSC. To demonstrate the capability of the proposed method, the experiment also compares the proposed scheme with the traditional TSF algorithm in time series landslide detection.

2. METHODOLOGY

This study aims to detect landslides using time series satellite images. The proposed method includes three major works: (1) image preprocessing; (2) time series preprocessing; and (3) landslide detection. The flowchart is shown as Figure 1.

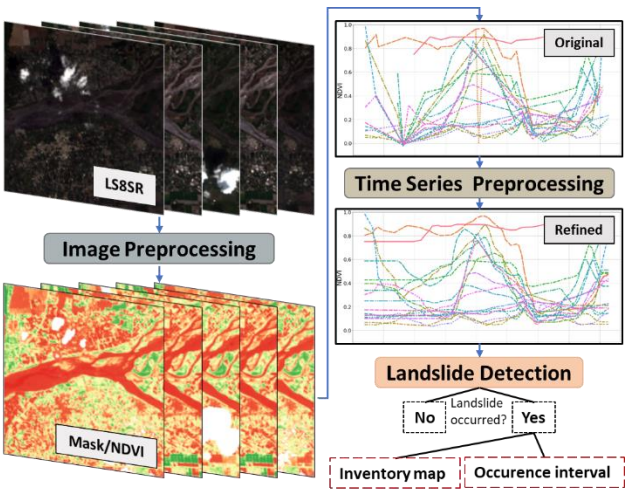

Figure 1. Workflow of the proposed method.

2.1 Image Preprocessing

The Google Earth Engine (GEE) is a cloud-based platform with massive remote sensing data and powerful cloud-computing capabilities (Gorelick et al., 2015). The GEE is designed for planetary-scale geospatial analysis. Therefore, large-scale and multi-temporal data can be easily retrieved by GEE. This study obtained multi-temporal and multispectral Landsat-8 (LS8) satellite images using GEE. We use the atmospherically corrected surface reflectance from the LS8 OLI/TIRS sensors to avoid atmospheric influences. In addition, the quality assessment (QA) bands generated using the CFMask (Foga et al., 2017) algorithm can be used to exclude cloud regions. Once the cloud mask for each image is established, the time series normalized difference vegetation index (NDVI) can be obtained by calculating band rationing.

$$NDVI = \frac{NIR - R}{NIR + R} \quad (1)$$

NDVI is a normalized index with a value between -1.0 and 1.0. NIR stands for near-infrared band and R for red band. High NDVI values about 0.6 to 0.9 correspond to dense vegetation; Moderate NDVI values about 0.2 to 0.5 may indicate sparse vegetation or senescent crop; An NDVI value lower than 0.1 may represent bare soil or rock (Brown, 2015). The image product and band information used in the study are shown in Table 1.

Table 1. LS8 band info.

Sensing time		Provider	Image Collection
2016/01/01-2018/12/31		USGS	LANDSAT/LC08/C01/T1_SR
Band	Resolution(m)	Wavelength	Description
B2	30	0.45 - 0.51 μm	Blue
B3	30	0.53 - 0.59 μm	Green
B4	30	0.64 - 0.67 μm	Red
B5	30	0.85 - 0.88 μm	NIR
BQA	30		QA Bitmask

2.2 Time Series Preprocessing

Landslides often occur in mountainous areas and usually cause sudden changes in land cover. The most common phenomenon is transforming vegetation area to bare soil (Deijns et al., 2020). The NDVI time series can be used to distinguish the land with and without a landslide in mountainous areas (Figure 2). Therefore, the NDVI time series can be applied to landslide detection. The time series preprocessing procedures include error elimination, Gaussian smoothing, and resampling.

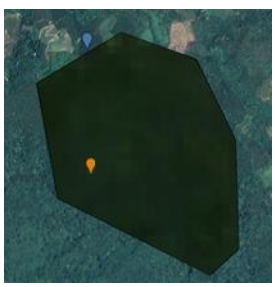

(a) 2017 LS8 RGB image

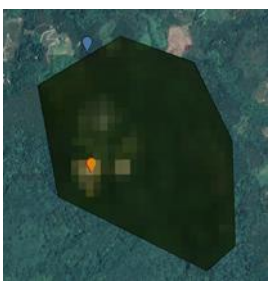

(b) 2018 LS8 RGB images

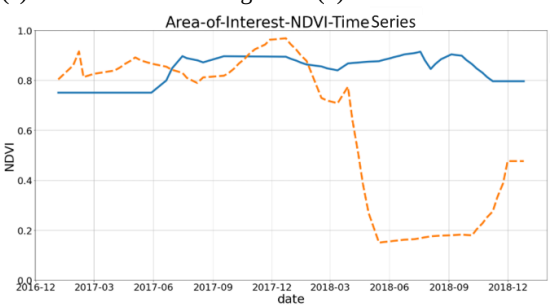

(c) NDVI time series of landslide and non-landslide (blue: non-landslide；orange: landslide)

Figure 2. Illustration of time series NDVI.

This contribution has been peer-reviewed. The double-blind peer-review was conducted on the basis of the full paper.
https://doi.org/10.5194/isprs-annals-V-3-2022-557-2022 | © Author(s) 2022. CC BY 4.0 License.

Error elimination mainly removes obvious errors in the series. A possible reason for the error is the thin clouds, which are more likely to not be detected by the CFMask algorithm. Therefore, an incorrect NDVI value (close to 0) may be computed because the area covered by the cloud is not entirely excluded. In this case, the value of that timestamp will be eliminated while the NDVI value is less than 0. Then, we apply Gaussian smoothing to reduce the effect of high-frequency noise. The last procedure of time series preprocessing is a cubic interpolation, which aims to regularize time series with different lengths. In this study, each time series was resampled to one value per week (53 timestamps per year). The visualization results of time series preprocessing are shown in Figure 3.

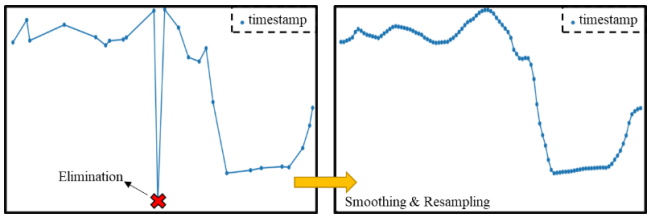

Figure 3. Time series preprocessing

2.3 Landslide Detection

TSF is an interval-based tree-ensemble classifier and the TSF classifier can be regarded as a random forest classifier for time series, which splits the time series into multiple random intervals. After extracting features (such as mean, standard deviation, and slope) in each interval, each decision tree is trained from the extracted features. Finally, ensemble learning is used to combine these weak classifiers to improve the accuracy of classification. The algorithm also introduces a new method for calculating information gain called Entrance gain, which is superior to the algorithm using Entropy gain (Deng et al., 2013). Furthermore, the TSF used the temporal importance curve to quantify the importance of different intervals for time series classification. The TSF algorithm is summarized as follows:

Algorithm 1 TSF Classifier

Input: A list of ***n*** cases with series length ***m***.
Parameters: number of trees ***s***, minimum length of an interval ***l***.
Assume forest **F** = $(F_1, F_2, \cdots, F_{s-1}, F_s)$
for i=1 to s **do**
  $t1 = rand(1, m - l)$
  $t2 = rand(t1 + l, m)$
  Split the series into $\sqrt{m}$ intervals by $t1$ and $t2$ timestamps
  Extract features (mean, std and slope) from each interval
  Train decision tree F_i on the extracted $3\sqrt{m}$ features
end for
Output Ensemble the trees with averaged probability estimates

Since the landslide behavior does not have a regular period, the time interval change from dense vegetation to bare land also varies for each landslide region. Therefore, this study applies an interval segmentation method based on local extrema to extract the discriminated local features of time series. This study proposed a simple and adaptive time series landslide algorithm called **landslide interval detection (LID)**. The LID algorithm detects landslide intervals from a time series with arbitrary length. The LID algorithm is based on two assumptions. The first is the need for high quality preprocessing procedures, such as error elimination, smoothing, and resampling. The second is to set reasonable parameters for the algorithm. The parameters required for LID include tolerance of local changes and NDVI threshold. The former is mainly used to identify the peaks and valleys within time series intervals. Once the local changes exceed the minimum threshold, it is regarded as a new peak/valley. The latter determines whether the time series between local extremes can be interpreted as a landslide. The details of LID are shown as the pseudo-code in Algorithm 2.

Algorithm 2 LID

Input: A time series ***S*** with length ***m***.
Parameters:
Min. relative change required to define a peak, thr_up
Min. relative change required to define a valley, thr_down
Min. NDVI to identify as pre-event data, vmin
Max. NDVI to identify as post-event data, vmax
Min. difference between pre- and post-event NDVI, vdiff
initialize trend (+1or -1), last_d = S[0], and a landslide interval list L
for i=2 to m **do**
  $d = S[i]$
  $r = d/\text{last}_d$
  if trend $= -1$ **then**
    if $r \geq$ thr_up **then**
      trend $= 1, \text{last}_d = d, \text{last}_i = i$
      if $S[\text{last}_{peak}] \geq$ vmin & $S[\text{last}_{peak}] - S[i-1] \geq$ vdiff **then**
        L.append($[\text{last}_{peak}, i-1]$)
      end if
    if $d < \text{last}_d$ **then**
      $\text{last}_d = d$ and $\text{last}_i = i$
    end if
  end if
  if trend $= 1$ **then**
    if $r \leq$ thr_down **then**
      trend $= -1, \text{last}_d = d,$ $\text{last}_i = i,$ and $\text{last}_{peak} = i - 1$
    end if
    if $d > \text{last}_d$ **then**
      $\text{last}_d = d$ and $\text{last}_i = i$
    end if
  end if
end for
output L

3. TRAINING AND TEST DATASETS

For the evaluation of time series landside classification algorithms, we selected well-defined training and test samples through a two-stage procedure. In the first stage, we obtained the landslide areas through the vector difference between the landslide inventory maps (provided by Forestry Bureau, Council of Agriculture, Executive Yuan, Taiwan) in the years 2016, 2017 and 2018. These landslide inventory maps were manually digitized by Formosat-2 multispectral satellite images with a spatial resolution of 8m. Most of the landslide polygons are small and fragmented. Therefore, if the LS8 images with 30m spatial resolution are calculated pixel-wise, mixed pixels will affect it. To ensure the correctness of the samples, we set two criteria to select suitable training and test regions for LS8: (1) The area of the vector difference $\geq 3600m^2$; and (2) The radius of the maximum inscribed circle of the polygon $\geq$ 30m. The center of the inscribed circle is the coordinates of the time series retrieval (Figure 4).

The yearly landslide inventory map does not provide the landslide occurrence time. The area obtained in the first stage contains some non-landslide areas. Therefore, we manually interpret the landslide by the geomorphic changes and the

difference between pre-/post-event optical images in the second stage. The time series retrieval is from 2016 to 2018, and a total of 149 time series per year are obtained for training and testing. The above procedure ensures that the acquired time series has indeed experienced landslides. In binary classification, non-landslide samples need to be generated to maximize the difference between landslide and non-landslide samples for classification. The non-landslide sample of this study is the hillside area that has not collapsed, including land that is always covered in vegetation and land that is always bare. We also manually selected 149 non-landslide samples to balance the number of landslide and non-landslide training samples.

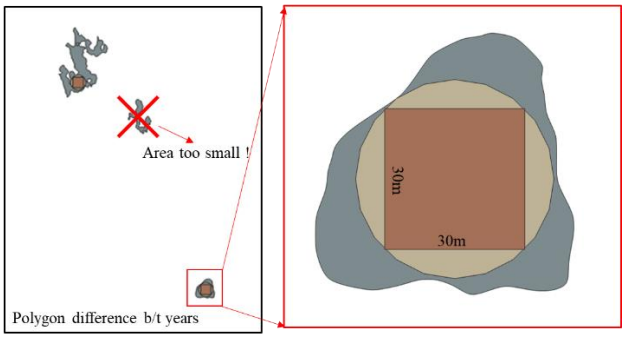

Figure 4. Coordinates selection for time series retrieval

4. EXPERIMENTS AND RESULTS

This section describes the experimental results from the two aforementioned methods (i.e., TSF and LID) and presents classification results on the same dataset. The time series used in both methods goes through the same preprocessing procedure. The TSF model needs to be trained. We used 80% of the dataset as training data, while the remaining 20% is used as independent test data. As a result, the training dataset has 238 time series, and the test dataset has 60 time series. The accuracy assessment is based on the same criteria, so LID uses the same test data as TSF. Figure 5 demonstrates the time series of test data with their label.

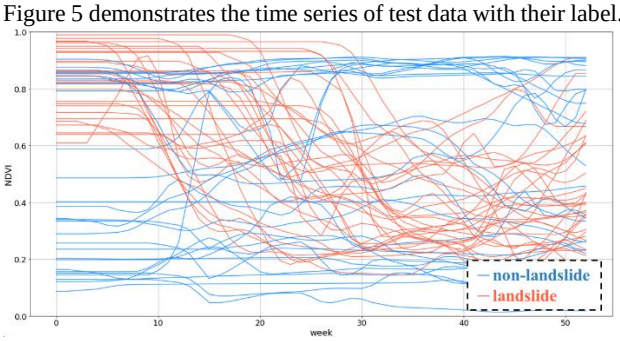

Figure 5. Time series of test data

4.1 Time Series Forest (TSF)

TSF calculates the features in different intervals by randomly splitting the time series and then performs the ensemble learning-based classification using the Random Forest algorithm. The parameters required for training the TSF classifier in this study are set as follows: (1) The number of decision trees is 300; (2) The minimum length of the interval is about one month, which is 4 timestamps in resampled series; (3) Bootstrap aggregation was applied when building decision trees (bootstrap=True); and (4) Estimate the generalization accuracy using out-of-bag error (oob_score=True). The confusion matrix computed by the prediction of test data is shown in Figure 6. There is only one misclassified case each for the non-landslide time series. All evaluation indicators (i.e., accuracy, precision, recall, F1-score, and Kappa values) show fairly good prediction results using the TSF algorithm (Table 2). However, by calculating the importance of each interval feature, it is found that the time series slope change is the most important feature in the TSF model (Figure 7).

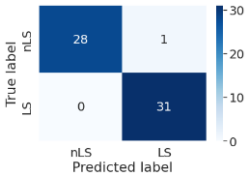

Figure 6. Confusion matrix of TSF

Table 2. Evaluation indicators

Accuracy	0.98
Precision	0.98
Recall	0.98
F1-score	0.98
Kappa	0.96

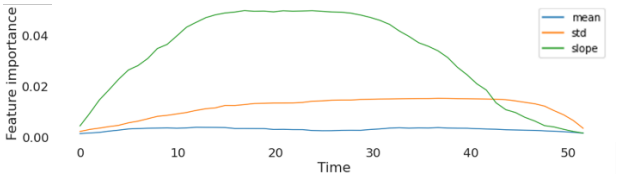

Figure 7. Interval-feature importance

4.2 Landslide Interval Detection (LID)

The LID algorithm assumes sudden vegetation change in the landslide region. This algorithm splits the time series into several intervals by indicating the peaks and valleys of the series. Once the trend of the next timestamp is opposite to the previous one and is greater than the minimum of the relative change, the timestamp may be indicated as a peak or a valley. As shown in Figure 8, the red points are the peaks or valleys of the time series; the black line is the connection between the local extremum and the starting point/end point of the series; the black dotted line is the non-landslide interval; the red line indicates the landslide interval using the proposed method. Two critical parameters need to be predefined in splitting intervals: the minimum values of the relative change required to define a peak or a valley. We determined the minimum values for the indication of a peak or a valley through extensive experiments to 0.2. The LID algorithm can be applied to time series of any length. In identifying landslide time series, two empirical parameters are set as follows: (1) A minimum NDVI value of 0.6 was used to filter peaks in the series. The purpose is to ensure that each detected landslide interval is covered by healthy vegetation in the early stage. (2) The second parameter is the minimum value of NDVI difference between selected intervals. The minimum value of difference is given as 0.31 by the minimum change in the landslide time series of training data. The hyperparameters used in this study are depicted in Table 3.

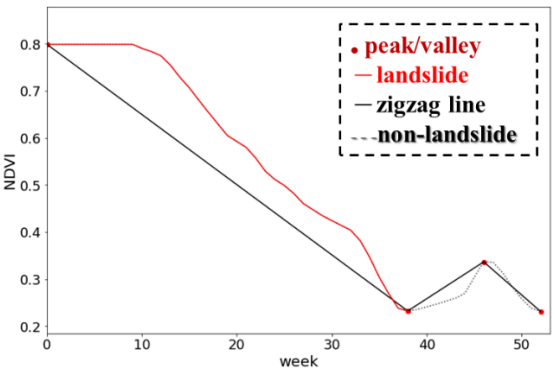

Figure 8. Illustration of landslide interval detection

Table 3. LID hyperparameters

Hyperparameters	value
thr_up	0.20
thr_down	0.20
v_{min}	0.60
v_{diff}	0.31

If the time series contains multiple landslides, each interval can also be found using the LID algorithm. The LID classification results were verified using the same test data as TSF. In the test data classification results, LID accurately predicts the label of each time series. The confusion matrix is shown in Figure 9, and the evaluation indicators are shown in Table 4.

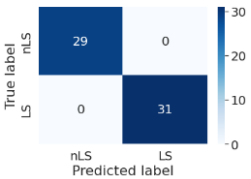

Figure 9. Confusion matrix of LID

Table 4. Evaluation indicators

Accuracy	1.00
Precision	1.00
Recall	1.00
F1-score	1.00
Kappa	1.00

4.3 Pixel-wise evaluation

Both TSF and LID achieved high accuracy for the test dataset. The accuracies of these two methods are similar in the test dataset, so we used the pretrained model to assess the performance of these two methods in a real case. The ground truth in the real case is manually digitized from 1.5m high-resolution bitemporal satellite images. The satellite images were taken on February 14, 2015 and March 3, 2016. The mean of the landslide area is $2738m^2$ which is about 3 pixels for Landsat-8. Which means, most landslide is relatively small for the Landsat-8 multispectral image. The distribution of the landslide is shown in Figure 9. The evaluation includes qualitative and quantitative analysis. The details of data analysis are provided in the following sections.

Figure 9. Landslide area location

4.3.1 Qualitative analysis

In the visual inspection, it is found that most of the areas detected by the TSF algorithm are rivers. The possible reason is that the river basin has undergone cover changes between the wet and dry periods. As a result, it was misclassified as a landslide. Although the LID method also made some mistakes, the number of detected landslides is relatively less than TSF. In the large landslide area, LID has better identification ability than TSF, as shown in the area selected by the yellow dotted line in Figure 10. In addition, it can be found that there are very few areas where the TSF predicted area overlaps the ground truth. The pretrained TSF model can only correctly extract very few landslides.

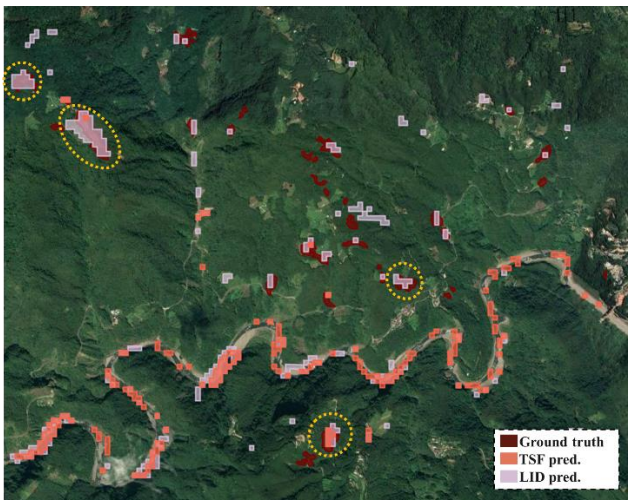

Figure 10. Visualization of classification results (real case)

4.3.2 Quantitative analysis

The quantitative analysis calculates the intersection over union (IoU) as a quality index. We first use the 20m DEM to simply calculate the slope to eliminate the misclassification of the drainage lines. Then IoU is calculated by calculating the ratio of union and intersection. If the IoU is greater than 0.5, it means that the landslide was successfully detected; if the IoU is less than 0.5, it means that the omission occurred. Only 3 out of 44 landslides were detected by the TSF algorithm, while the LID algorithm successfully indicated 18 landslides. In view of the 30m spatial resolution of LS8, we also analyzed the relationship between different landslide areas and omission error (Table 5). For landslides that are smaller than 3600m^2 (i.e., 4pixels for LS8), the omission errors for both TSF and LID were larger than 0.77. But for the landslides that are larger than 3600m^2, the omission errors for TSF and LID were 0.92 and 0.15, respectively. As a result, we found that the overall performance using TSF is poor regardless of the landslide area. The discriminative ability of LID is much better than TSF in large landslide areas.

Table 5. Relationship between area and omission error

	Omission error: landslide smaller than 3600m^2	Omission error: Landslide larger than 3600m^2
TSF	29/31 (0.94)	12/13 (0.92)
LID	24/31 (0.77)	2/13 (0.15)

5. CONCLUSIONS AND FUTURE WORKS

This study proposed an interval-based time series classification method called LID. Besides, we also performed a preliminary comparison of LID with another interval-based algorithm (i.e., TSF). Both TSF and LID show high accuracy (≥ 0.98) for training and test datasets. However, under pixel-wise classification with a real case scenario, the overall accuracy of TSF is only 0.07. LID has an overall accuracy of about 0.41, and its accuracy is higher than 0.85 in large areas ($\geq 3600m^2$). TSF is a data-driven supervised classification that relies on

discriminative pre-labeled data. Due to the relatively small dataset used in this study, the TSF classification accuracy in real cases is insufficient. In other words, it may represent that the pre-trained TSF classifier is not a general model for pixel-wise landslide time series. By contrast, the experimental results of LID are better than TSF in real cases with pixel-wise classification and have better detection ability in large-scale landslides. It is worth mentioning that the omission error of LID in a large-scale landslide is about 0.15, which can roughly identify the landslide area and its occurrence interval. Future work will expand the time series dataset and introduce multivariate time series data to improve discrimination ability. Moreover, higher spatial resolution optical satellites, such as Sentinel-2, will be used to reduce the omission in small-scale landslides.

ACKNOWLEDGMENTS

This research was partially supported by the Ministry of Interior (111CCL030C) and Ministry of Science and Technology of Taiwan.

REFERENCES

Bagnall, A., Lines, J., Bostrom, A., Large, J., & Keogh, E. 2017. The great time series classification bake off: a review and experimental evaluation of recent algorithmic advances. Data mining and knowledge discovery, 31(3), 606-660.

Baydogan, M. G., & Runger, G. 2016. Time series representation and similarity based on local autopatterns. Data Mining and Knowledge Discovery, 30(2), 476-509.

Baydogan, M. G., Runger, G., & Tuv, E. 2013. A bag-of-features framework to classify time series. IEEE transactions on pattern analysis and machine intelligence, 35(11), 2796-2802.

Brown, J. 2015. NDVI, the Foundation for Remote Sensing Phenology. USGS Remote Sensing Phenology: Vegetation Indices.

Chen, T., Trinder, J. C., & Niu, R. 2017. Object-oriented landslide mapping using ZY-3 satellite imagery, random forest and mathematical morphology, for the Three-Gorges Reservoir, China. Remote sensing, 9(4), 333.

Cheng, G., Guo, L., Zhao, T., Han, J., Li, H., & Fang, J. 2013. Automatic landslide detection from remote-sensing imagery using a scene classification method based on BoVW and pLSA. International Journal of Remote Sensing, 34(1), 45-59.

Danneels, G., Pirard, E., & Havenith, H. B. 2007. Automatic landslide detection from remote sensing images using supervised classification methods. In 2007 IEEE international geoscience and remote sensing symposium (pp. 3014-3017). IEEE.

Deijns, A. A., Bevington, A. R., van Zadelhoff, F., de Jong, S. M., Geertsema, M., & McDougall, S. 2020. Semi-automated detection of landslide timing using harmonic modelling of satellite imagery, Buckinghorse River, Canada. International Journal of Applied Earth Observation and Geoinformation, 84, 101943.

Deng, H., Runger, G., Tuv, E., & Vladimir, M. 2013. A time series forest for classification and feature extraction. Information Sciences, 239, 142-153.

Foga, S., Scaramuzza, P. L., Guo, S., Zhu, Z., Dilley Jr, R. D., Beckmann, T., ... & Laue, B. 2017. Cloud detection algorithm comparison and validation for operational Landsat data products. Remote sensing of Environment, 194, 379-390.

Furuta, R., & Tomiyama, N. 2008. A Study of Detection of Landslide Disasters due to the Pakistan Earthquake using ALOS data. PRISM, 2008.

Gorelick, N., Hancher, M., Dixon, M., Ilyushchenko, S., Thau, D., & Moore, R. 2017. Google Earth Engine: Planetary-scale geospatial analysis for everyone. Remote sensing of Environment, 202, 18-27.

Guzzetti, F., Mondini, A. C., Cardinali, M., Fiorucci, F., Santangelo, M., & Chang, K. T. 2012. Landslide inventory maps: New tools for an old problem. Earth-Science Reviews, 112(1-2), 42-66.

Handwerger, A. L., Jones, S. Y., Huang, M. H., Amatya, P., Kerner, H. R., & Kirschbaum, D. B. 2020. Rapid landslide identification using synthetic aperture radar amplitude change detection on the Google Earth Engine. Natural Hazards and Earth System Sciences Discussions, 1-24.

Herrera Herrera, M. 2019. Landslide Detection using Random Forest Classifier. Master of Science in Geomatics at Delft University of Technology.

Konishi, T., & Suga, Y. 2017. Extraction of damaged area caused by debris flows in Hiroshima using COSMO-SkyMed images. In Active and Passive Microwave Remote Sensing for Environmental Monitoring (Vol. 10426, p. 1042604). International Society for Optics and Photonics.

Müller, M. 2007. Dynamic time warping. Information retrieval for music and motion, 69-84.

Plank, S., Twele, A., & Martinis, S. 2016. Landslide mapping in vegetated areas using change detection based on optical and polarimetric SAR data. Remote Sensing, 8(4), 307.

Schäfer, P. 2015. The BOSS is concerned with time series classification in the presence of noise. Data Mining and Knowledge Discovery, 29(6), 1505-1530.

Shen, C. 2015. Analysis of detrended time-lagged cross-correlation between two nonstationary time series. Physics Letters A, 379(7), 680-687.

Shibayama, T., & Yamaguchi, Y. 2014. A landslide detection based on the change of scattering power components between multi-temporal PolSAR data. In 2014 IEEE geoscience and remote sensing symposium (pp. 2734-2737). IEEE.

Ye, L., & Keogh, E. 2009. Time series shapelets: a new primitive for data mining. In Proceedings of the 15th ACM SIGKDD international conference on Knowledge discovery and data mining (pp. 947-956).